High-temperature rate constant measurements for OH + xylenes

ARTICLE *in* COMBUSTION AND FLAME · MARCH 2015

Impact Factor: 3.08 · DOI: 10.1016/j.combustflame.2015.02.001

3 AUTHORS, INCLUDING:

Ahmed Elwardany

King Abdullah University of Science and Te…

29 PUBLICATIONS **257** CITATIONS

SEE PROFILE

Jihad A. Badra

Saudi Arabian Oil Company

28 PUBLICATIONS **60** CITATIONS

SEE PROFILE

Combustion and Flame xxx (2015) xxx–xxx

Contents lists available at ScienceDirect

Combustion and Flame

journal homepage: www.elsevier.com/locate/combustflame

High-temperature rate constant measurements for OH + xylenes

Ahmed Elwardany [a,b], Jihad Badra [a,c], Aamir Farooq [a,*]

[a] Clean Combustion Research Centre, Division of Physical Sciences and Engineering, King Abdullah University of Science and Technology (KAUST), Thuwal 23955-6900, Saudi Arabia
[b] Mechanical Engineering Department, Faculty of Engineering, Alexandria University, Alexandria 21544, Egypt
[c] Saudi Aramco Research and Development Center, Fuel Technology R&D Division, Dhahran 31311, Saudi Arabia

ARTICLE INFO

Article history:
Received 30 December 2014
Received in revised form 2 February 2015
Accepted 2 February 2015
Available online xxxx

Keywords:
Xylene
Hydroxyl radical
Shock tube
Laser absorption
Rate constant

ABSTRACT

The overall rate constants for the reactions of hydroxyl (OH) radicals with *o*-xylene (k_1), *m*-xylene (k_2), and *p*-xylene (k_3) were measured behind reflected shock waves over 890–1406 K at pressures of 1.3–1.8 atm using OH laser absorption near 306.7 nm. Measurements were performed under pseudo-first-order conditions. The measured rate constants, inferred using a mechanism-fitting approach, can be expressed in Arrhenius form as:

$$k_1 = 2.93 \times 10^{13} \exp(-1350.3/T)\ \text{cm}^3\ \text{mol}^{-1}\ \text{s}^{-1} \quad (890\text{–}1406\ \text{K})$$
$$k_2 = 3.49 \times 10^{13} \exp(-1449.3/T)\ \text{cm}^3\ \text{mol}^{-1}\ \text{s}^{-1} \quad (906\text{–}1391\ \text{K})$$
$$k_3 = 3.5 \times 10^{13} \exp(-1407.5/T)\ \text{cm}^3\ \text{mol}^{-1}\ \text{s}^{-1} \quad (908\text{–}1383\ \text{K})$$

This paper presents, to our knowledge, first high-temperature measurements of the rate constants of the reactions of xylene isomers with OH radicals. Low-temperature rate-constant measurements by Nicovich et al. (1981) were combined with the measurements in this study to obtain the following Arrhenius expressions, which are applicable over a wider temperature range:

$$k_1 = 2.64 \times 10^{13} \exp(-1181.5/T)\ \text{cm}^3\ \text{mol}^{-1}\ \text{s}^{-1} \quad (508\text{–}1406\ \text{K})$$
$$k_2 = 3.05 \times 10^{9} \exp(-400/T)\ \text{cm}^3\ \text{mol}^{-1}\ \text{s}^{-1} \quad (508\text{–}1391\ \text{K})$$
$$k_3 = 3.0 \times 10^{9} \exp(-440/T)\ \text{cm}^3\ \text{mol}^{-1}\ \text{s}^{-1} \quad (526\text{–}1383\ \text{K})$$

1. Introduction

Traditional transportation fuels are complex mixtures of different hydrocarbons including n-/iso-/cyclo-alkanes, olefins, and aromatics [1]. Approximately 30% and 20% of gasoline and diesel fuels, respectively, are composed of aromatics [1,2]. Some aromatic molecules, such as toluene, tri-methyl benzene, and xylene, are considered necessary constituents of surrogate fuel formulations [3–5]. Aromatics are found in the initial fuel composition and produced during the oxidation of large aliphatic fuels [2]. Because of their lower reactivity in comparison to n-/iso-alkanes, aromatics are also used as antiknock additives to enhance gasoline octane rating [6]. Hence, studying the kinetic targets (e.g., ignition delay times, species time histories, and reaction rate constants) of aromatics has attracted attention from several researchers [1,3,6–15].

The reaction of hydroxyl (OH) radicals with alkanes, alkenes, and aromatics is one of the primary oxidation pathways for these molecules under atmospheric and combustion conditions. A few studies have investigated the reaction between OH and aromatics, but these studies either targeted lower temperatures or focused on the first two smallest aromatics, benzene and toluene. Perry et al. [13] measured the rate constant of the reaction between OH radicals and benzene, toluene, xylene isomers, and trimethyl benzene isomers at temperatures of 296–473 K using flash photolysis and the resonance fluorescence technique. Tully et al. [14] also used flash photolysis and the resonance fluorescence technique to measure the rate constants for the reaction of OH radicals with benzene and toluene over a wider temperature range of 213–1150 K. Recently, Vasudevan et al. [15] measured the rate constant for OH + toluene behind reflected shock waves using OH laser absorption near 306.7 nm for temperatures ranging between 911 and 1389 K. A recent experimental study on the rate constants for reactions of benzene and toluene with OH radicals was conducted by

* Corresponding author.
E-mail address: aamir.farooq@kaust.edu.sa (A. Farooq).

http://dx.doi.org/10.1016/j.combustflame.2015.02.001
0010-2180/

Seta el al. [2] using a shock tube and pulsed laser-induced fluorescence for temperatures in the range of 908–1736 K.

The high-temperature H-abstraction reactions of OH radicals with the three xylene isomers can be expressed by the following:

$$OH + o\text{-xylene}(1,2\ \text{dimethyl benzene}) \rightarrow \text{Products} \quad (R1)$$

$$OH + m\text{-xylene}(1,3\ \text{dimethyl benzene}) \rightarrow \text{Products} \quad (R2)$$

$$OH + p\text{-xylene}(1,4\ \text{dimethyl benzene}) \rightarrow \text{Products} \quad (R3)$$

Most previous studies of these reactions have been limited to room temperature conditions [16–20], with the exception of three studies that measured rate constants at higher temperatures (296–970 K). As mentioned earlier, Perry et al. [13] measured the rate constants of R1–R3 for a temperature range of 296–473 K. Mehta et al. [21] used the relative rate and discharge flow mass spectrometry technique with 1,4 dioxane as the reference compound over a range of 240–340 K to measure the rate constants of R1–R3 reactions. Nicovich et al. [12] investigated the kinetics of these reactions using the flash photolysis and resonance fluorescence technique over a temperature range of 250–970 K.

In this work, the rate constants for R1–R3 are measured at combustion relevant temperatures (890–1406 K). Measurements are performed under pseudo-first-order conditions with the help of narrow line-width absorption of OH radicals near 306.7 nm. This study reports the first rate-constant measurements for R1–R3 at temperatures higher than 970 K. Arrhenius expressions are derived for the studied temperature range and then extended to lower temperatures using previously published data.

2. Experimental set up

All experiments were performed behind reflected shockwaves in a high-purity stainless steel shock tube facility. The inner surface of the shock tube is honed and electro-polished to reduce boundary layers and trapped impurities. The driven section is 9 m long, while the driver section length can be varied to a maximum of 9 m; both sections have an inner diameter of 14.2 cm. Further details of the shock tube can be found elsewhere [22]. The incident shock velocity was determined (±0.1%) using five PCB (Model 113B26) piezo-electric pressure transducers (PZT) spaced over the last 1.3 m of the driven section. The shock velocity at the endwall was determined by extrapolating the measured velocity. The preshock pressure and temperature, P_1 and T_1, are measured using a high-accuracy Baratron pressure transducer and a K-type thermocouple, respectively. Reflected shock conditions, P_5 and T_5, were calculated using standard normal-shock relations and thermochemical data taken from the Sandia thermodynamics database [23].

Gas mixtures were prepared manometrically in a uniformly heated (50 °C) stainless steel mixing tank equipped with a magnetic stirrer assembly. *Tert*-butyl hydroperoxide (*t*BHP), a well-known precursor of OH radicals [15], is thermally decomposed to produce OH radicals. Previous work draws a comparison between *t*BHP and gaseous nitric acid as hydroxyl radical precursors [2,15]. High-purity He (99.999%), supplied by Abdullah Hashim Gases (AHG), is used as the driver gas. Test gas mixtures are prepared using research grade argon (99.999%) supplied by AHG, 70% *t*BHP aqueous solution and *o*-, *m*- or, *p*-xylene (⩾99%) supplied by Sigma Aldrich. Repeated freeze–pump–thaw cycles were used to further purify the xylenes.

OH radicals were measured using the well-characterized R1 (5) line of the OH A–X (0, 0) band. UV light was tuned to the peak of the absorption line near 306.6868 nm. Visible red light near 613.4 nm (~1 W) was generated in a Matisse ring dye laser from Sirah by pumping a solution of 0.75 g/L Rhodamine B dye in ethylene glycol with a 10 W, 532 nm, cw beam produced by the Millenia Prime laser from Spectra Physics. The visible red beam was then sent to a CW Spectra Physics Wave Train frequency doubler that generates UV light (~100 mW) near 306.7 nm. A beam splitter is used to send a fraction of the UV beam to a reference detector and the remaining fraction to pass through the shock tube at an optical location 2 cm from the endwall (see Fig. 1). Hydroxyl radical mole fractions were determined quantitatively using the Beer–Lambert law, $I/I_0 = \text{Exp}(-k_v X_{OH} P_5 L)$, where I and I_0 are the transmitted and incident laser intensities, respectively; k_v is the absorption coefficient calculated following the work of Herbon [24]; P_5 is the total reflected shock pressure (atm); and L is the optical path length (14.2 cm). The overall estimated uncertainty in the measured OH mole fraction, X_{OH}, is approximately ±3%, mainly due to the uncertainty in reflected shock temperature (±0.7%) and absorption cross section.

3. Results and discussion

3.1. High-temperature rate-constant measurements

The overall rate constants for the reactions of *o*-, *m*-, and *p*-xylene with OH (R1), (R2), (R3) were measured behind reflected shockwave under pseudo-first-order conditions over a temperature range of 890–1406 K and pressures ranging between 1.3 and 1.8 atm. The experiments were performed using varying initial fuel concentrations/*t*BHP: 130 ppm *o*-xylene/10 ppm *t*BHP, 120 ppm *m*-xylene/9 ppm *t*BHP, and 220 ppm *p*-xylene/17 ppm *t*BHP. Argon was used as the diluent bath gas.

Hydroxyl radical decay was simulated using the mechanism by Narayanaswamy et al. [25], which was developed for the oxidation of toluene, styrene, ethylbenzene, 1,3-dimethylbenzene (*m*-xylene), and 1-methylnaphthalene. The *m*-xylene submechanism was validated against ignition delay time and burning velocity measurements of *m*-xylene. The TBHP ((CH3)3–CO–OH) chemistry set (described in [22,26–28]) is included in the base mechanism of Narayanaswamy et al. [25] to simulate OH radical formation.

$$TBHP((CH_3)_3\text{—}CO\text{—}OH) \rightarrow OH + \textit{tert}\text{-Butoxy}((CH_3)_3\text{—}CO) \quad (R4)$$

$$\textit{tert}\text{-Butoxy} \rightarrow CH_3 + CH_3COCH_3 \quad (R5)$$

$$OH + TBHP \rightarrow H_2O + O_2 + \textit{tert}\text{-}C_4H_9 \quad (R6)$$

$$OH + TBHP \rightarrow H_2O + HO_2 + \textit{iso}\text{-}C_4H_8 \quad (R7)$$

TBHP decomposes almost instantaneously to form an OH radical and a *tert*-butoxy radical that subsequently decomposes to form acetone and methyl radical. Moreover, the OH radical can attack TBHP to produce water and other products [22,27,28]. Thermodynamic properties of the newly introduced species, including TBHP and a *tert*-butoxy radical, were extracted from the thermodynamic database from Goos et al. [29] and the updated thermodynamic parameters of OH radicals were taken from Herbon et al. [30]. Rate constants for R4, R6, and R7 reactions were obtained from Pang et al. [31], and the rate constant for reaction R5 was taken from Choo and Benson [32].

A representative OH sensitivity analysis for a mixture of 120-ppm *m*-xylene (written in the base mechanism as A1CH$_3$CH$_3$) with 9-ppm *t*BHP (and 24-ppm H_2O vapor) and balanced argon is shown in Fig. 2 at 1024 K and 1.54 atm. All simulations were performed using CHEMKIN PRO [33] with constant volume and internal energy (constant UV) constraints. OH sensitivity is calculated as $S = (\partial X_{OH}/\partial k_i) \times (k_i/X_{OH})$, where X_{OH} is the OH radical mole fraction and k_i is the rate constant of the ith reaction. Sensitivity

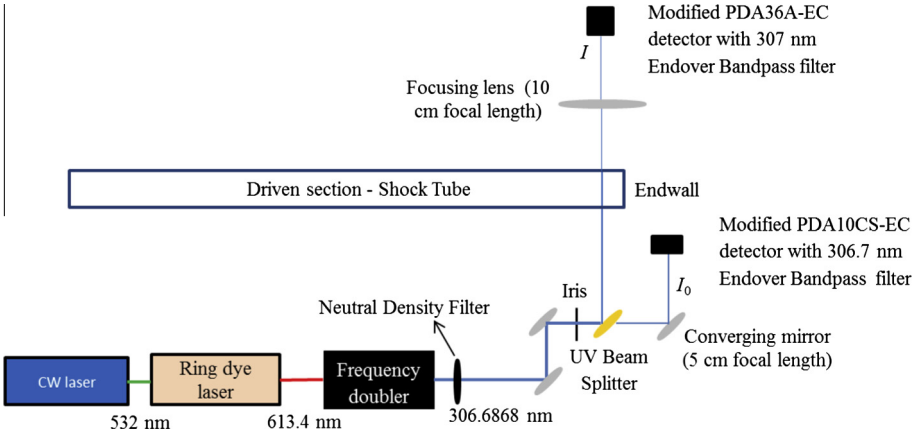

Fig. 1. A schematic of the optical setup for OH radical absorption in the shock tube.

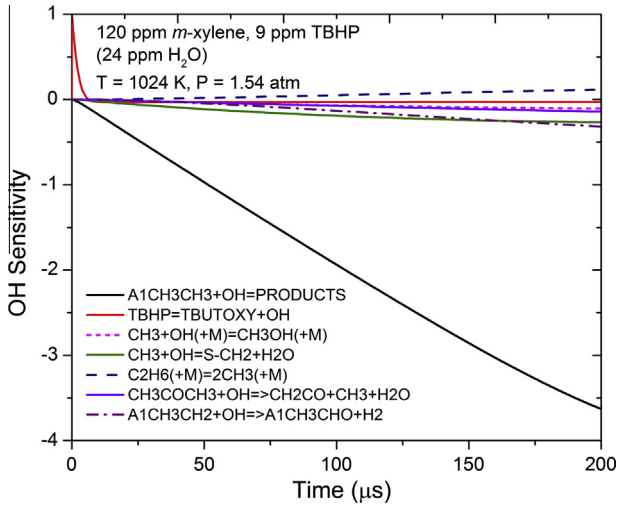

Fig. 2. Hydroxyl radical sensitivity for the rate-constant measurement of OH + *m*-xylene ($A1CH_3CH_3$) at 1024 K and 1.54 atm.

analysis shows that reaction of *m*-xylene and OH (R2) is dominant over the entire time domain of the experiments (~100 μs). Early on (e.g., less than 10 μs), there is minor evidence of interference from the TBHP decomposition reaction, and the influence of this interference on OH radical decay is negligible. Later on, secondary reactions begin to show some interference. Because of recent recommendations and measurements, rate constants of the interfering reactions were updated in the base mechanism. One of the important interfering reactions is the reaction of methyl groups with OH radicals:

$$CH_3 + OH \rightarrow S\text{-}CH_2 + H_2O \quad (RS1)$$

The rate constant for the RS1 reaction was updated with the measured values proposed by Pang et al. [31]. The rate constant of the decomposition of ethane

$$C_2H_6(+M) \rightarrow 2CH_3(+M) \quad (RS2)$$

was updated in the base mechanism as measured by Oehlschlaeger et al. [34]. The rate constant of the decomposition of methanol

$$CH_3OH(+M) \rightarrow CH_3 + OH \quad (RS3)$$

was updated with the values measured by Srinivasan et al. [35]. Rate constants of the other reactions shown in the sensitivity analysis were used as given by the base mechanism.

The base mechanism developed by Narayanaswamy et al. [25] was modified by adding corresponding OH reactions for o-xylene and p-xylene. These reactions and their rate constants were taken from Battin-Leclerc et al. [36] (see Table S1 in the Supplementary Material). The sensitivity analyses for the representative o-xylene and p-xylene mixtures shown in Figs. S2 and S3 (Supplementary Material), respectively, illustrate that the dominant interfering reactions are RS1–RS3. The rate constants of these reactions are modified in the base mechanism, as discussed above.

A typical measured OH time-history profile is shown in Fig. 3 for the reaction of OH with *m*-xylene at a representative condition of 1024 K and 1.54 atm. Representative OH profiles at lower (955 K) and higher (1328 K) temperatures are shown in Fig. S1 (Supplementary Material). Time zero is determined by matching the peak of the simulated OH radical profile (using the mechanism) with the measured OH radical peak. The experimental slow rise of OH before $t = 0$ (for $T > 1000$ K) is attributed to the relatively low bandwidth (760 kHz) of the detector. The detector bandwidth can be set as high as 10 GHz but the signal-to-noise ratio decreases with increase in bandwidth. At lower temperatures (<1000 K), the experimental slow rise of OH radicals disappears because the used detector bandwidth is high enough to adequately capture the increase in OH radicals. Figure 3 shows a notch, a schlieren spike, in the measured trace close to the peak that is caused by density gradients; it is small due to the relatively small change in density at this temperature. At high temperatures, as shown in Fig. S1(b), a more prominent schlieren spike can be seen. Figure 3(a) demonstrates that OH radical decay does not reach zero at later times (>500 μs) because of the interference caused by the absorption of light near 306 nm by xylene. To account for this, the OH radical profiles were shifted down to reach zero ppm at long times. This is a reasonable approach because xylenes have broadband UV spectra and the concentration of xylene remains almost constant during the course of the experiment.

Measured OH radical decay profiles were analyzed using two methods: (i) the first-order or exponential-fitting method and (ii) the mechanism-fitting method. The first-order rate constant, k_{1st}, is calculated from the slope of the linear line when ln[OH] is plotted as a function of time, as shown in Fig. 3(c). The second-order rate constant can then be calculated as: $k_{OH+Fuel} = k_{1st}/[F]_0$, where $[F]_0$ is the initial fuel concentration. For the conditions shown in Fig. 3, a first-order rate constant of 16890 s^{-1} is obtained followed by the second-order rate constant at 7.79×10^{12} cm^3 $mole^{-1}$ s^{-1}. Using the best-fit profile from the Narayanaswamy et al. [25] mechanism, the rate constant is calculated at 6.37×10^{12} cm^3 $mole^{-1}$ s^{-1}, as shown in Fig. 3(b). The rate-constant values calculated using the first-order method and mechanism-fitting

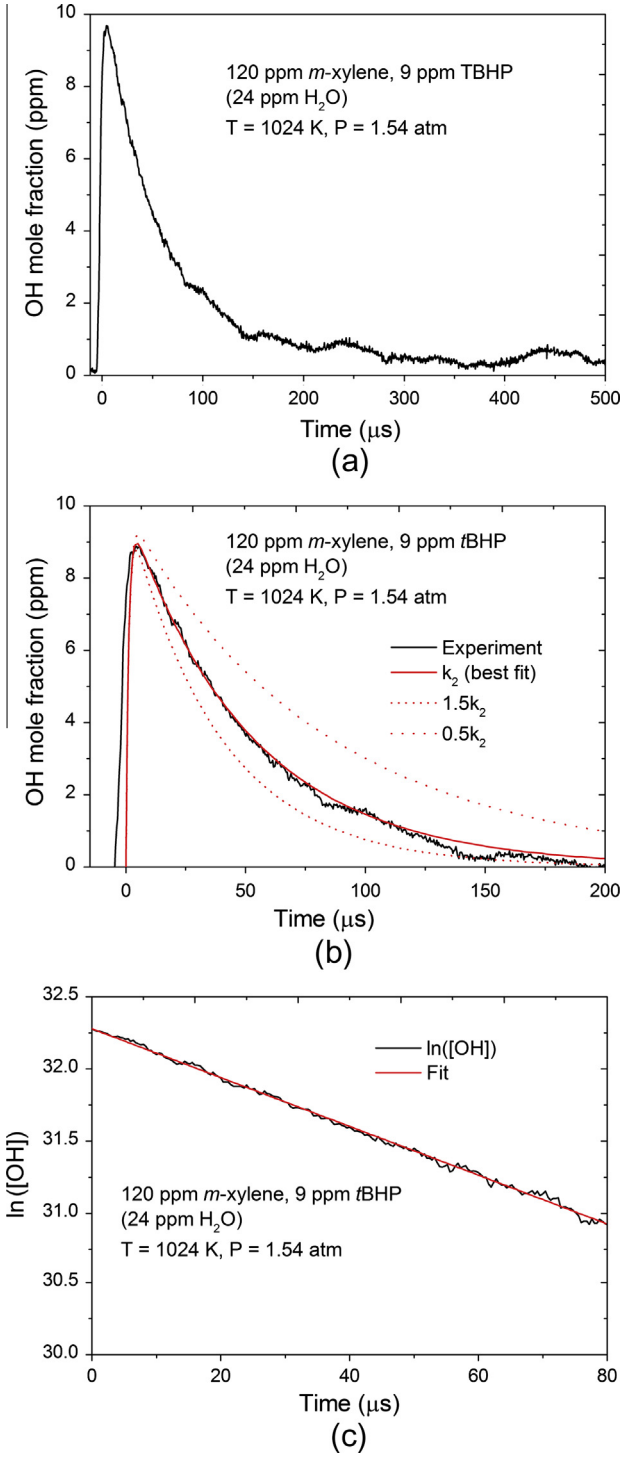

Fig. 3. (a) A temporal profile of OH radical decay for a 120-ppm *m*-xylene/9-ppm *t*BHP/Ar mixture at 1024 K and 1.54 atm. (b) Best-fit simulated rate constant and perturbations of ±50%. (c) The first-order rate-constant determination.

method were also compared at other temperatures. A difference of approximately 20% between the two methods is within the experimental uncertainty. Representative OH radical profiles and corresponding exponential fits for the reaction of OH radicals with *o*-xylene and *p*-xylene are given in the Supplementary Material (Figs. S4 and S5).

The mechanism-fitting methodology is preferred here because it includes the effects of secondary reactions. Measured rate constants for reactions R1–R3, extracted using the mechanism fitting method, are shown on an Arrhenius plot in Fig. 4. Although the rate constants of reactions R1–R3 are within 20–30%, a systematic trend is discernable among the three xylene isomers. For example, the rate coefficients scale directly with the position of the second methyl group, where p-xylene (1,4-dimethylbenzene) exhibits the highest rate-constant values because the two methyl groups are furthest apart. The high sensitivity of these measurements enabled us to uncover these small, yet expected, differences in the reactivity of the three xylene isomers. The measured values of rate constants for reactions R1–R3, extracted using both exponential-fit and mechanism-fitting methods, are summarized in Tables S2–S4 (Supplementary material) and can be expressed in Arrhenius form as follows:

$$k_{OH+o\text{-xylene}} = 2.1 \times 10^{13} \exp(-1067.7/T)\ \text{cm}^3\ \text{mol}^{-1}\ \text{s}^{-1}$$
(890–1406K) (Exponential fit)

$$k_{OH+o\text{-xylene}} = 2.93 \times 10^{13} \exp(-1350.3/T)\ \text{cm}^3\ \text{mol}^{-1}\ \text{s}^{-1}$$
(890–1406 K) (Mechanism fit)

$$k_{OH+m\text{-xylene}} = 2.47 \times 10^{13} \exp(-1140.6/T)\ \text{cm}^3\ \text{mol}^{-1}\ \text{s}^{-1}$$
(906–1391 K) (Exponential fit)

$$k_{OH+m\text{-xylene}} = 3.49 \times 10^{13} \exp(-1449.3/T)\ \text{cm}^3\ \text{mol}^{-1}\ \text{s}^{-1}$$
(906–1391 K) (Mechanism fit)

$$k_{OH+p\text{-xylene}} = 2.7 \times 10^{13} \exp(-1177.1/T)\ \text{cm}^3\ \text{mol}^{-1}\ \text{s}^{-1}$$
(908–1383 K) (Exponential fit)

$$k_{OH+p\text{-xylene}} = 3.5 \times 10^{13} \exp(-1407.5/T)\ \text{cm}^3\ \text{mol}^{-1}\ \text{s}^{-1}$$
(908–1383 K) (Mechanism fit).

Detailed uncertainty analyses were performed for the three measured rate constants. The following sources of errors were considered: mixture composition (±5%); the OH radical absorption coefficient (±3%); reflected shock temperature (±0.7%); wavemeter reading (±0.002 cm^{-1}); fitting the experimental profiles (±5%); locating time zero (±1.0 μs); and the rate constants of $CH_3 + OH = S\text{-}CH_2 + H_2O$ (uncertainty factor = 2), CH3OH(+M)= CH3 + OH (+M) (uncertainty factor = 2), and C_2H_6 (+M) = $2CH_3$(+M) (±20%). The effect of each of these error sources on the measured rate constant was calculated separately. The uncertainties were then combined in a root-sum-squared method to get the overall uncertainties of ±19% at 1040 K with 1.6 atm, ±22% at 1024 K with 1.54 atm, and ±24% at 1146 K with 1.49 atm for k_1, k_2, and k_3, respectively.

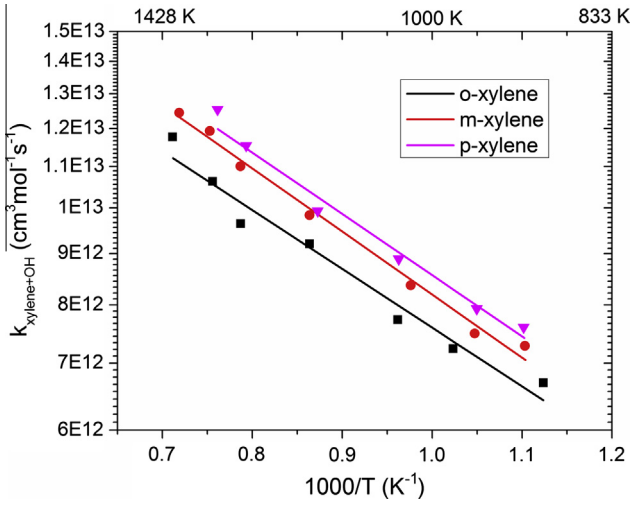

Fig. 4. An Arrhenius plot for OH + xylene → Products for the three xylene isomers.

3.2. Extension to low temperatures

Nicovich et al. [12] measured the rate constants of R1–R3 from low to moderate temperatures (250–970 K). They noticed three primary channels for the reaction of OH radicals with xylene isomers: at temperatures lower than 320 K, the addition of OH radicals to benzene rings dominates; at temperatures higher than 500 K, the H-abstraction from CH_3 groups dominates; and at an intermediate temperature range (320–500 K), the behavior was complicated and nonexponential decay of the OH radicals was observed. Here, rate constants measured are combined with values from Nicovich et al. [12] for temperatures higher than 500 K, where H-abstraction dominates. Rate constants measured here and by Nicovich et al. [12] for reaction R1 (o-xylene + OH) are presented in Fig. 5. For the overlapping temperature range, our measured values are about 30% lower than those from Nicovich et al. [12]. Although this difference is within the experimental uncertainty of the two studies, we believe that our values are more accurate owing to the use of a highly sensitive OH radical absorption diagnostic. Figure 5 also shows rate coefficient values adopted in the kinetic mechanism of Battin-Leclerc et al. [36], which seem to be anchored to the data from Nicovich et al. [12]. A fit to the two experimental data sets gives the following Arrhenius expression (shown as a "red" line in Fig. 5):

$$k_1 = 2.64 \times 10^{13} \exp(-1181.5/T)\ \mathrm{cm^3\ mol^{-1}\ s^{-1}} \quad (508\text{–}1406\ \mathrm{K})$$

Similarly, current high-temperature measurements for *m*-xylene + OH (R2) are combined with data from Nicovich et al. [12] and are shown in Fig. 6. The two data sets cover a temperature range of 508–1391 K. A fit to the two experimental data sets gives the following Arrhenius expression:

$$k_2 = 3.05 \times 10^{9} \exp(-400/T)\ \mathrm{cm^3\ mol^{-1}\ s^{-1}} \quad (508\text{–}1391\ \mathrm{K})$$

Figure 6 also shows rate coefficient values adopted in the mechanisms by Battin-Leclerc et al., Narayanaswamy et al., and Gudiyella et al. [25,36,37]. Rate constant values used in the mechanism by Battin-Leclerc et al. overpredict the measured values by approximately 25% over the entire temperature range. Rate constant values used in the mechanism from Gudiyella et al. agree with our measurements at low temperatures (<1000 K) but overpredict the high-temperature data by about 10%. Additionally, the values used in the Narayanaswamy et al. mechanism are slower at low temperatures (<1100 K) and faster at high temperatures.

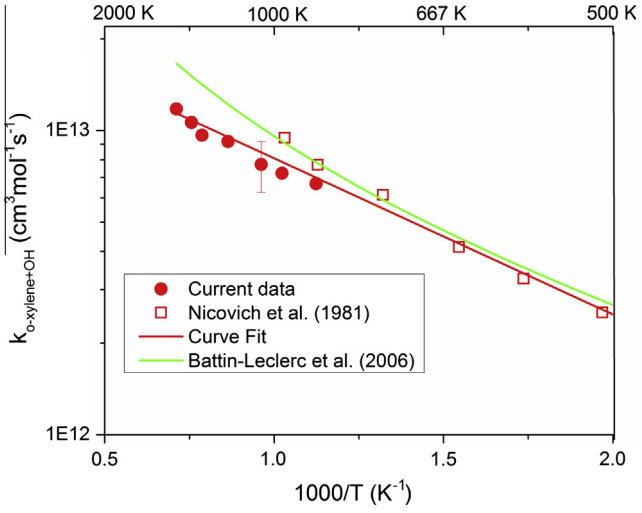

Fig. 5. An Arrhenius plot for OH + *o*-xylene for a temperature range of 508–1406 K. The red curve is the fit to experimental data from this work and Nicovich et al. [12]. (For interpretation of the references to color in this figure legend, the reader is referred to the web version of this article.)

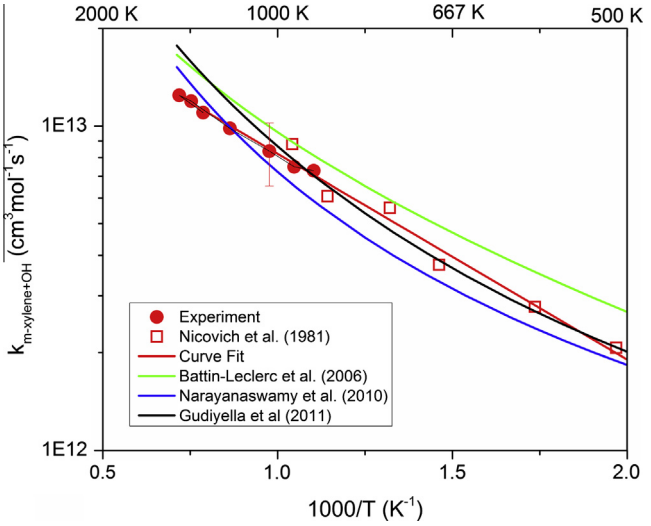

Fig. 6. An Arrhenius plot for OH + *m*-xylene for a temperature range of 508–391 K. The red line is the fit to experimental data from this work and Nicovich et al. [12]. (For interpretation of the references to color in this figure legend, the reader is referred to the web version of this article.)

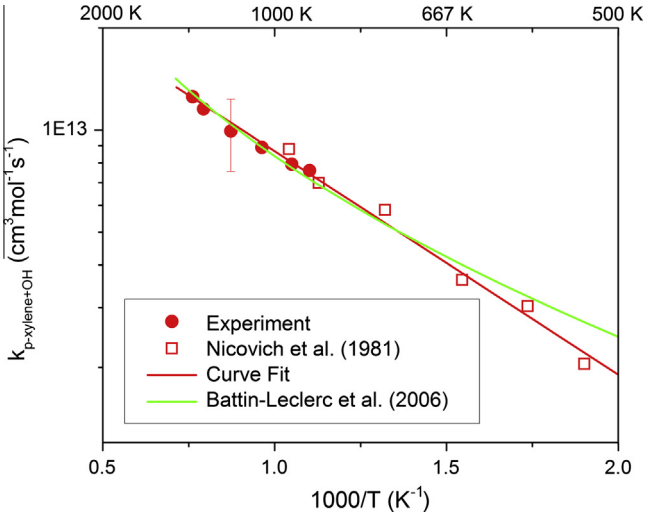

Fig. 7. An Arrhenius plot for OH + p-xylene for a temperature range of 526–1383 K. The red line represents a fit of experimental data from this work and Nicovich et al. [12]. (For interpretation of the references to color in this figure legend, the reader is referred to the web version of this article.)

Figure 7 illustrates the reaction of *p*-xylene with OH radicals (R3) by presenting our high-temperature measurements along with data from Nicovich et al. [12]. In addition, the estimated values adopted in the mechanism by Battin-Leclerc et al. are presented which agree with the measured values over the entire temperature range. A fit to the two experimental data sets results in the following Arrhenius expression:

$$k_3 = 3.0 \times 10^{9} \exp(-440/T)\ \mathrm{cm^3\ mol^{-1}\ s^{-1}} \quad (526\text{–}1383\ \mathrm{K})$$

4. Conclusions

The overall rate constants for the reaction of hydroxyl radicals with *o*-xylene (k_1), *m*-xylene (k_2), and *p*-xylene (k_3) were measured

behind reflected shockwaves over a temperature range of 890–1406 K using OH radical laser absorption. This work presents the first high-temperature rate constant measurements for reactions of xylene isomers with OH radicals. The largest rate constants were measured for *p*-xylene, followed by *m*-xylene and *o*-xylene. This trend is consistent with the expected reactivity of the xylene isomers as a result of the position of methyl branching on the benzene ring. These high-temperature data are combined with previous low-temperature measurements to provide Arrhenius expressions that are valid over a wide temperature range.

Acknowledgments

Research reported in this publication was supported by the King Abdullah University of Science and Technology (KAUST) and by Saudi Aramco under the FUELCOM program.

Appendix A. Supplementary material

Supplementary data associated with this article can be found, in the online version, at http://dx.doi.org/10.1016/j.combustflame.2015.02.001.

References

[1] B. Gauthier, D. Davidson, R. Hanson, Combust. Flame 139 (4) (2004) 300–311.
[2] T. Seta, M. Nakajima, A. Miyoshi, J. Phys. Chem. A 110 (15) (2006) 5081–5090.
[3] M. Fikri, J. Herzler, R. Starke, C. Schulz, P. Roth, G. Kalghatgi, Combust. Flame 152 (1) (2008) 276–281.
[4] M. Mehl, J.Y. Chen, W.J. Pitz, S.M. Sarathy, C.K. Westbrook, Energy Fuels 25 (11) (2011) 5215–5223.
[5] G. Kukkadapu, K. Kumar, C.-J. Sung, M. Mehl, W.J. Pitz, Combust. Flame (2012).
[6] K. Brezinsky, Prog. Energy Combust. Sci. 12 (1) (1986) 1–24.
[7] G. Mittal, C.-J. Sung, Combust. Flame 150 (4) (2007) 355–368.
[8] V. Vasudevan, D. Davidson, R. Hanson, Proc. Combust. Inst. 30 (1) (2005) 1155–1163.
[9] J. Herzler, M. Fikri, K. Hitzbleck, R. Starke, C. Schulz, P. Roth, G.T. Kalghatgi, Combust. Flame 149 (1–2) (2007) 25–31.
[10] D. Davidson, B. Gauthier, R. Hanson, Proc. Combust. Inst. 30 (1) (2005) 1175–1182.
[11] M. Hartmann, I. Gushterova, M. Fikri, C. Schulz, R. Schießl, U. Maas, Combust. Flame 158 (1) (2011) 172–178.
[12] J. Nicovich, R. Thompson, A. Ravishankara, J. Phys. Chem. 85 (20) (1981) 2913–2916.
[13] R. Perry, R. Atkinson, J.N. Pitts Jr., J. Phys. Chem. 81 (4) (1977) 296–304.
[14] F. Tully, A. Ravishankara, R. Thompson, J. Nicovich, R. Shah, N. Kreutter, P. Wine, J. Phys. Chem. 85 (15) (1981) 2262–2269.
[15] V. Vasudevan, D.F. Davidson, R.K. Hanson, J. Phys. Chem. A 109 (15) (2005) 3352–3359.
[16] D. Hansen, R. Atkinson, J. Pitts Jr., J. Phys. Chem. 79 (17) (1975) 1763–1766.
[17] G.J. Doyle, A.C. Lloyd, K. Darnall, A.M. Winer, J.N. Pitts Jr., Environ. Sci. Technol. 9 (3) (1975) 237–241.
[18] R.A. Kenley, J.E. Davenport, D.G. Hendry, J. Phys. Chem. 85 (19) (1981) 2740–2746.
[19] T. Ohta, T. Ohyama, Bull. Chem. Soc. Jpn. 58 (10) (1985) 3029–3030.
[20] F. Kramp, S.E. Paulson, J. Phys. Chem. A 102 (16) (1998) 2685–2690.
[21] D. Mehta, A. Nguyen, A. Montenegro, Z. Li, J. Phys. Chem. A 113 (46) (2009) 12942–12951.
[22] J. Badra, A.E. Elwardany, F. Khaled, S.S. Vasu, A. Farooq, Combust. Flame (2013).
[23] R. Kee, F. Rupley, J. Miller, The Chemical Thermodynamic Data Base, Report No. SAND87-8215B.UC-4, Sandia National Laboratory; 1987.
[24] J.T. Herbon, Shock Tube Measurements of CH3 + O2 Kinetics and the Heat of Formation of the OH Radical, Stanford University, 2004.
[25] K. Narayanaswamy, G. Blanquart, H. Pitsch, Combust. Flame 157 (10) (2010) 1879–1898.
[26] K.-Y. Lam, D.F. Davidson, R.K. Hanson, J. Phys. Chem. A 116 (23) (2012) 5549–5559.
[27] S.S. Vasu, J. Zádor, D.F. Davidson, R.K. Hanson, D.M. Golden, J.A. Miller, J. Phys. Chem. A 114 (32) (2010) 8312–8318.
[28] S.S. Vasu, Z. Hong, D.F. Davidson, R.K. Hanson, D.M. Golden, J. Phys. Chem. A 114 (43) (2010) 11529–11537.
[29] E. Goos, A. Burcat, B. Ruscic, Argonne National Lab., Rept. ANL-05/20, Argonne, IL, 2005.
[30] J.T. Herbon, R.K. Hanson, D.M. Golden, C.T. Bowman, Proc. Combust. Inst. 29 (1) (2002) 1201–1208.
[31] G.A. Pang, R.K. Hanson, D.M. Golden, C.T. Bowman, Z. Phys. Chem. 225 (11–12) (2011) 1157–1178.
[32] K.Y. Choo, S.W. Benson, Int. J. Chem. Kinet. 13 (9) (1981) 833–844.
[33] R.J. Kee, F.M. Rupley, J.A. Miller, in: Reaction Design Inc: San Diego, CA, 2010.
[34] M.A. Oehlschlaeger, D.F. Davidson, R.K. Hanson, Proc. Combust. Inst. 30 (1) (2005) 1119–1127.
[35] N. Srinivasan, M.-C. Su, J. Michael, J. Phys. Chem. A 111 (19) (2007) 3951–3958.
[36] F. Battin-Leclerc, R. Bounaceur, N. Belmekki, P. Glaude, Int. J. Chem. Kinet. 38 (4) (2006) 284–302.
[37] S. Gudiyella, T. Malewicki, A. Comandini, K. Brezinsky, Combust. Flame 158 (4) (2011) 687–704.